



## Molecular Crystals and Liquid Crystals Science and Technology. Section A. Molecular Crystals and Liquid Crystals

Publication details, including instructions for authors and  
subscription information:

<http://www.tandfonline.com/loi/gmcl19>

### FT Pulsed and CW EPR Studies of Stable Molecular Spin Crystals

Daisuke Shiomi <sup>a</sup> , Kazunobu Sato <sup>b</sup> , Yoshio Teki <sup>a</sup> , Takeji Takui <sup>b</sup> ,  
Koichi Itoh <sup>a</sup> , Koichi Tanaka <sup>c</sup> & Fumio Toda <sup>c</sup>

<sup>a</sup> Department of Material Science, Osaka City University, Sumiyoshi-ku, Osaka, 558, Japan

<sup>b</sup> Department of Chemistry, Osaka City University, Sumiyoshi-ku, Osaka, 558, Japan

<sup>c</sup> Department of Industrial Chemistry and Applied Chemistry, Ehime University, Matsuyama, 790, Japan

Version of record first published: 24 Sep 2006.

To cite this article: Daisuke Shiomi , Kazunobu Sato , Yoshio Teki , Takeji Takui , Koichi Itoh , Koichi Tanaka & Fumio Toda (1995): FT Pulsed and CW EPR Studies of Stable Molecular Spin Crystals, Molecular Crystals and Liquid Crystals Science and Technology. Section A. Molecular Crystals and Liquid Crystals, 271:1, 173-182

To link to this article: <http://dx.doi.org/10.1080/10587259508034050>

PLEASE SCROLL DOWN FOR ARTICLE

Full terms and conditions of use: <http://www.tandfonline.com/page/terms-and-conditions>

This article may be used for research, teaching, and private study purposes. Any substantial or systematic reproduction, redistribution, reselling, loan, sub-licensing, systematic supply, or distribution in any form to anyone is expressly forbidden.

The publisher does not give any warranty express or implied or make any representation that the contents will be complete or accurate or up to date. The accuracy of any instructions, formulae, and drug doses should be independently verified with primary sources. The publisher shall not be liable for any loss, actions, claims, proceedings, demand, or costs or damages whatsoever or howsoever caused arising directly or indirectly in connection with or arising out of the use of this material.

## FT PULSED AND CW EPR STUDIES OF STABLE MOLECULAR SPIN CRYSTALS

DAISUKE SHIOMI,<sup>1</sup> KAZUNOBU SATO,<sup>2</sup> YOSHIO TEKI,<sup>1</sup>  
TAKEJI TAKUI,<sup>2</sup> KOICHI ITOH,<sup>1</sup> KOICHI TANAKA,<sup>3</sup> AND FUMIO TODA<sup>3</sup>  
<sup>1</sup>Department of Material Science and <sup>2</sup>Department of Chemistry, Osaka City  
University, Sumiyoshi-ku, Osaka 558, Japan; <sup>3</sup>Department of Industrial  
Chemistry and Applied Chemistry, Ehime University, Matsuyama 790, Japan

**Abstract** The potential application of time domain EPR spectroscopy to an organic molecular spin system was examined, particularly focusing upon quantum spin transient nutation phenomena. A nitronyl nitroxide-based biradical with an excited triplet state ( $S=1$ ), *p*-phenylenebis( $\alpha$ -nitronylnitroxide), was adopted as a simple model system for studying the nutation spectroscopy which enables us to discriminate between  $S \geq 1$  and  $S=1/2$  states. In the low temperature region below 10 K, an  $S=1$  spin of the thermally excited biradical molecule and an  $S=1/2$  spin of an impurity molecule were found to coexist in the crystalline solid state of *p*-phenylenebis( $\alpha$ -nitronylnitroxide). Field-swept echo-detected EPR spectra reproduced the cw spectra of the biradical powder. Echo-detected nutation spectra exhibited two distinct maxima of the echo intensity at the nutation frequencies expected for  $S=1$  and  $S=1/2$  spins, indicating that the biradical solid was identified to be a mixture of the  $S=1$  and  $S=1/2$  species as expected from the static susceptibility and crystal structure analysis of the biradical. The nutation method based on FT pulsed EPR spectroscopy was demonstrated to be complementary to conventional cw EPR and susceptibility measurements.

## INTRODUCTION

One of the most noticeable characteristics of molecular spin solids is that spin states with different spin quantum numbers  $S$  are thermally accessible, the magnetic interaction between unpaired electrons being comparable with the thermal energy  $k_B T$ . This feature sometimes gives rise to difficulties in investigating their magnetic interaction from the microscopic viewpoint by using cw EPR (EPR with field modulation) and static susceptibility: These conventional methods have disadvantages in discriminating between  $S \geq 1$  and  $S=1/2$  spins, particularly for strongly exchange-coupled magnetic materials such as paramagnetic assemblages and organic high-spin polymers. In the present study, the potential application of time domain EPR spectroscopy to such complicated spin systems has been examined, focusing upon quantum spin transient nutation phenomena. We demonstrate that the nutation method based on FT pulsed EPR

spectroscopy enables us to identify the effective spin quantum number  $S$  of the spin assemblage in the molecular solid. The method can be complementary to conventional cw EPR and static susceptibility measurements.

### A SIMPLE MODEL SYSTEM FOR THE NUTATION SPECTROSCOPY

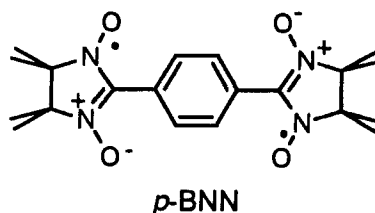
The theoretical basis for the transient spin nutation was first developed in NMR and NQR spectroscopy.<sup>1-9</sup> Nutation spectroscopy is based on spin resonance to measure the spin Hamiltonian in terms of the rotating frame. In the presence of a static field  $B_0$  and a microwave field  $B_1$  perpendicular to  $B_0$ , the spin magnetization precesses around the effective field  $B_{\text{eff}} = [(B_0 - \omega_{\text{MW}}/\gamma)^2 + B_1^2]^{1/2}$  ( $\gamma$ : gyromagnetic ratio) in the frame rotating at the microwave frequency  $\omega_{\text{MW}}$ . When the pulse microwave field  $B_1$  is applied for a period  $t_p$ , the on-resonance ( $\omega_{\text{MW}} = \gamma B_0$ ) magnetization precesses to the angle  $t_p \times \gamma B_1$ . The magnetization starts to undergo free induction decay (FID) just after the  $B_1$  field is turned off. This precession in the rotating frame is a transient nutation in the classical vector-spin picture. The nutation frequency  $\omega_N$  is  $\gamma B_1$  for  $S=1/2$  under the on-resonance condition.

For nutation of spin  $S \geq 1$ , a quantum mechanical treatment of density matrix formulation has to be invoked. The detailed discussion on the nutation frequency  $\omega_N$  of  $S \geq 1$  quantum spin system has been presented in the literature.<sup>10-12</sup> Only a brief description of  $\omega_N$  is given here. For  $S \geq 1$ , the  $\omega_N$  value under the on-resonance condition is dependent on the magnitude of the  $B_1 \cdot g \cdot S$  term ( $H_1$ ) relative to that of the fine structure term ( $H_D$ ),  $S \cdot D \cdot S$ , in the spin Hamiltonian: For vanishing  $H_D$  or  $H_D \ll H_1$ , the ensemble of spins  $S \geq 1$  nutates at the frequency of  $\omega_1 = \gamma B_1$  under the on-resonance condition; the frequency  $\omega_N$  is independent of  $S$ . For non-vanishing  $H_D$ , the nutation is modified by  $H_D$  and is not describable by a single frequency. In the extreme limit of  $H_D \gg H_1$ , on the other hand, the nutation frequency  $\omega_N$  is expressed as

$$\omega_N = \omega_1 [S(S+1) - M_S(M_S-1)]^{1/2} \quad (1)$$

for the allowed EPR transition between the spin sublevels  $|M_S-1\rangle$  and  $|M_S\rangle$ . Thus, the spin quantum number  $S$  and  $M_S$  can be identified in the nutation spectrum. This is the methodological essence of the nutation spectroscopy which enables us to discriminate between different  $S$  values in the molecular solid.

We adopt here a nitronyl nitroxide-based biradical with an excited triplet state



( $S=1$ ), *p*-phenylenebis( $\alpha$ -nitronylnitroxide), abbreviated to *p*-BNN, as the model compound. For this compound, the crystal structure and static paramagnetic susceptibility have been well characterized:<sup>14–16</sup> The susceptibility of *p*-BNN measured in the powder sample exhibited a maximum around 65 K and approaches zero at lower temperature.<sup>14</sup> The observed susceptibility was reproduced in terms of a thermal equilibrium between a singlet ( $S=0$ ) ground state and an excited triplet state with an energy gap of  $2J/k_B = -106$  K which describes antiferromagnetic interaction between two  $S=1/2$  spins in the molecule. From the X-ray crystal structure analysis of *p*-BNN,<sup>14,16</sup> the intermolecular magnetic interaction can be regarded as being small: the N–O groups of the *p*-BNN molecule, where the spin density is concentrated, are located far apart from those of the adjacent molecules. From the X-ray and susceptibility results, the biradical molecules can be approximated to be magnetically isolated to each other at low temperature

A small upturn of susceptibility below 10 K has been observed.<sup>14</sup> This would be due to a nitronyl nitroxide monoradical ( $S=1/2$ ) impurity (about 1 mol % of the biradical) generated in the synthesis procedure and incorporated in the lattice of the biradical crystal. Thus, both  $S=1$  and  $S=1/2$  species are expected to coexist in the crystalline solid, providing us with a simple model for the nutation study on a molecular spin solid containing different  $S$  species.

## EXPERIMENTAL

Field-swept echo and echo-detected nutation spectra for the *p*-BNN powder were recorded on a Bruker ESP380 FT EPR spectrometer with a dielectric cavity of tunable  $Q=100\sim 5000$ . The temperature ranging from 4.0 up to 20.0 K was controlled by using a Bruker helium-flow cryostat and an Oxford ITC4 temperature controller. The microwave pulse was amplified by a 1 kW traveling wave tube amplifier. The cw EPR spectra were measured using a Bruker ESP300 X-band EPR spectrometer equipped with an Oxford helium-flow cryostat. The *p*-BNN powder sample was prepared by the reported method.<sup>17</sup>

## CW EPR SPECTRA

At room temperature, an exchange-narrowed single line at  $g\sim 2.0$  was observed for the *p*-BNN powder. On lowering the temperature, the single line split into several lines as

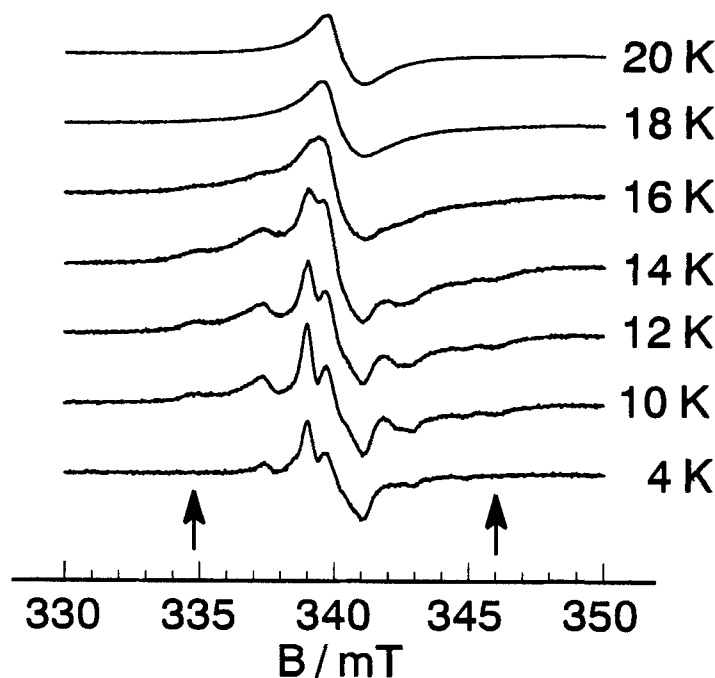


FIGURE 1 CW EPR spectra of the *p*-BNN powder. The arrows indicate the canonical-orientation transitions attributed to the thermally excited triplet state of *p*-BNN.

shown in Figure 1. The spectral profile observed below 16 K was apparently similar to that of phenylnitronylnitroxide monoradical ( $S=1/2$ ) measured in a glassy solution<sup>18</sup> except for two peripheral peaks indicated by the arrows in Figure 1. The spectral pattern for the monoradical has been explained in terms of the hyperfine coupling of an  $S=1/2$  spin with two equivalent nitrogen nuclei ( $I=1$ ).<sup>18</sup> The  $S=1/2$  monoradical impurity predominantly contributes to the powder spectra of *p*-BNN at low temperature. EPR signals from the excited triplet state of *p*-BNN should be superimposed on the intense  $S=1/2$  signal. The two peripheral peaks, which are not disturbed by the  $S=1/2$  signal, can be assigned to the canonical-orientation peaks appearing in the fine-structure spectrum from the excited triplet state of *p*-BNN. The separation of these two peaks is consistent with the fine structure splitting  $2|D| = 11 \text{ mT}$  ( $= 0.010 \text{ cm}^{-1}$ ) reported for a glassy solution of *p*-BNN.<sup>17</sup>

## PULSED EPR SPECTRA

The nutation experiments can be made by either observing the spin echo signal or free induction decay (FID) signal in the time domain by incrementing the duration time  $t_p$  of the microwave excitation pulse. Spin echo or FID signal intensity reflects the magnetization in the  $xy$ -plane of the rotating frame ( $z$ //static field) just after the application of the microwave excitation pulse. The pulse sequence for the echo-detected nutation experiment is schematically illustrated in Figure 2(a).

The free induction signal of  $p$ -BNN decayed rapidly and exhibited a poor signal/noise (S/N) ratio in the detection period; the transverse relaxation time was estimated to be 17 nanoseconds at 20 K assuming the single exponential decay of FID. At lower temperatures, no FID signal was detected on our pulse spectrometer with the resonator dead time of about 100 nanoseconds. On the other hand, the spin echo signals appeared below 20 K and the signal increased in intensity to a satisfactory S/N ratio with decreasing temperature. Our nutation experiments were performed by the echo-detected method in the temperature range between 4 K and 10 K.

### Field-swept echo-detected EPR spectra

Spin echo phenomena can be observed for a spin system which is subject to an inhomogeneous line-broadening, i.e., dephasing of homogeneous spin packets in the rotating frame.<sup>19</sup> When the echo-detected nutation is measured in order to discriminate between different  $S$ 's, it is necessary to ascertain whether the echo signal has contributions from all the spin states examined. For this purpose, echo-detected EPR spectra were measured for  $p$ -BNN.

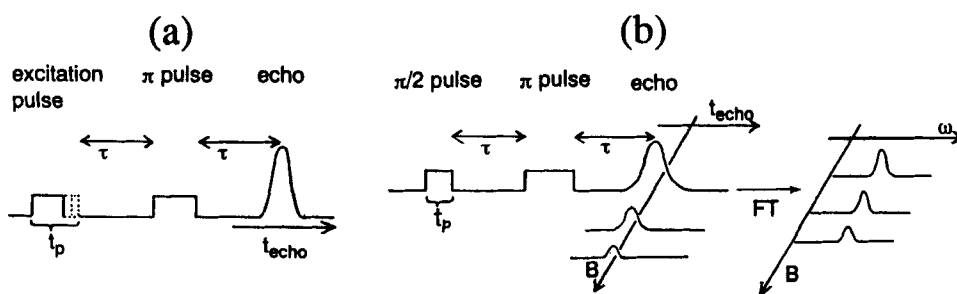


FIGURE 2 Pulse sequence scheme for echo-detected nutation (a) and field-swept echo-detected EPR (b) experiments.  $t_p$  and  $t_{echo}$  denote the duration time of microwave excitation pulse and the acquisition time for echo signal, respectively. The echo signal was monitored with incrementing  $t_p$ , i.e., the turning angle of the magnetization from the thermal equilibrium position (parallel to the static field).

When the excitation bandwidth  $\approx 1/t_p$  ( $t_p$ : the duration time of the microwave excitation pulse) is smaller than the line width of a structured EPR spectrum due to hyperfine or fine structure, the echo intensity should be a good measure of the magnetization at a particular static magnetic field.<sup>20</sup> Therefore, by detecting the echo signals with sweeping the static field, we can reconstruct an EPR spectrum as a function of the static field  $B$  (Figure 2(b)).

Figure 3(a) shows a two-dimensional representation of field-swept echo signals as a function of the static field  $B$  and the acquisition time  $t_{\text{echo}}$  measured for the  $p$ -BNN powder at 4.0 K. Fourier transformation of this time-domain spectrum along the  $t_{\text{echo}}$ -axis yields a frequency-domain spectrum as shown in Figure 3(b). Intense peaks appear only at zero MHz in the Fourier transformed spectrum. This means that only the on-resonance portion at each static field was selectively detected with a narrow excitation bandwidth. In fact, the application of an excitation pulse with  $t_p < 24$  nanoseconds gave rise to side bands at about 40 MHz running parallel to the field axis. The side bands are assignable to EPR transitions adjacent to the on-resonance transition giving the zero MHz signal. The separation of 40 MHz ( $= 1.4$  mT) corresponds to the hyperfine splitting of the monoradical.<sup>18</sup>

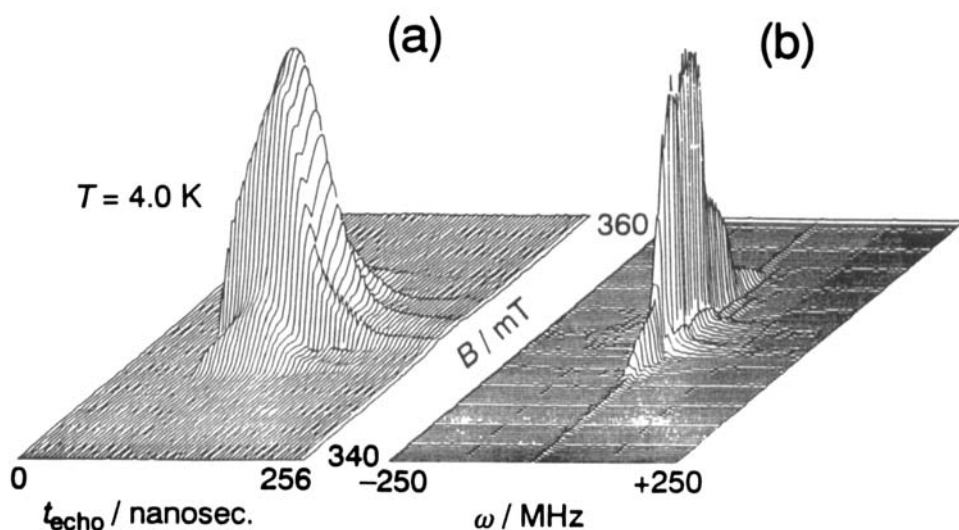


FIGURE 3 (a) Two-dimensional representation of the echo-detected EPR spectrum measured for the  $p$ -BNN powder at 4.0 K. (b) Frequency domain EPR spectrum obtained from the Fourier transformation of the time-domain spectrum in (a).

A slice at zero MHz of the Fourier-transformed spectrum is shown in Figure 4. The first derivative curve of the zero MHz slice reproduces the cw spectrum, although the weak peripheral peaks are absent in the curve. When the weak signal at 356 mT in the cw spectrum was pumped with the excitation pulse of  $t_p > 32$  nanoseconds, weak spin echo signal was observed. Considering that the  $t_p$  value corresponds to the excitation bandwidth smaller than 31 MHz (1.1 mT), which is rather small compared with the field separation between the weak peripheral peak and the adjacent  $S=1/2$  signal, the disappearance of the peripheral peaks in the zero MHz-slice spectrum resulted from the low S/N ratio of the echo signal.

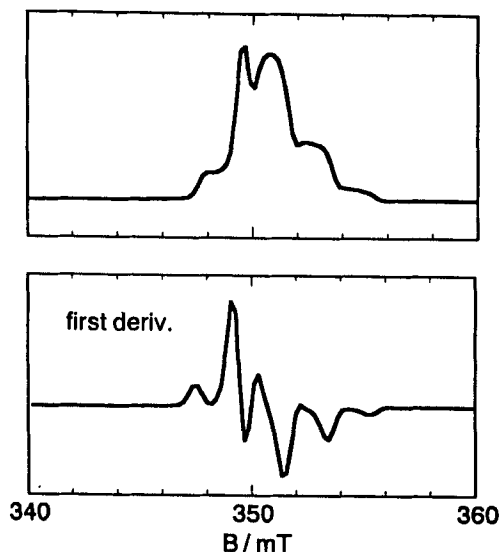


FIGURE 4 Echo-detected EPR spectrum of the *p*-BNN powder obtained as a slice at zero MHz of the frequency-domain spectrum in FIGURE 3(b).

It is concluded from the above results that the echo signal has the contribution both from the  $S=1/2$  and  $S=1$  species. Both the  $S=1/2$  impurity molecules and the thermally excited  $S=1$  molecules are microscopically distributed and hence isolated in the crystalline solid, leading to the inhomogeneous broadening. The present experiment for *p*-BNN has shown the capability of the nutation study by the echo-detected method.

### Nutation Spectra

The microwave field in the nutation experiments for *p*-BNN was applied so that the extreme limit condition of  $H_1 \ll H_D$  was fulfilled; the field amplitude  $B_1$  was much smaller than the fine structure splitting,  $2|D| = 11$  mT. The field amplitude  $B_1$  was calibrated with respect to the microwave power ( $\propto B_1^2$ ) by using the nutation frequency measured on an  $S=1/2$  radical (DPPH). The nutation frequencies calculated for  $S=1/2$  ( $M_S = -1/2 \leftrightarrow +1/2$  transition) and  $S=1$  ( $M_S = \pm 1 \leftrightarrow 0$  transitions) from Equation (1) are listed in Table I for the extreme limit condition.

Figure 5 shows a two-dimensional representation of one-dimensional Fourier-transformed nutation signals  $S(\omega_N, t_{\text{echo}})$ . The echo signals  $S(t_p, t_{\text{echo}})$  (not shown) have been Fourier-transformed along the  $t_p$ -axis into the frequency ( $\omega_N$ )-domain power



TABLE I Nutation frequencies calculated for  $S=1/2$  and  $S=1$  species under the present experimental condition.

$T$ (K)	microwave power (arb. units)	$\omega_N(S=1/2)$ (MHz)	$\omega_N(S=1)$ (MHz)
4.0~8.0	1	7.9	11
10.0	+ 5 dB	14	19

spectra. In the nutation experiments, the static magnetic field was set at the center of the cw spectra with the complicated structure due to the  $S=1/2$  and  $S=1$  species. Between 4.0 and 10.0 K, two distinct maxima of the echo signal intensity were observed along the  $\omega_N$ -axis as shown in Figure 5. The frequencies of these maxima agreed well with the calculated ones listed in Table I. Furthermore, these frequencies varied in proportion to  $B_1$ , indicating that the nutation along the effective field  $B_{\text{eff}}=B_1$  in the rotating frame was observed. From these results, it is concluded that the  $p$ -BNN powder at low temperature was determined to be a mixture of  $S=1/2$  and  $S=1$  species by the nutation experiments. This conclusion is consistent with the susceptibility result.

It should be noted that the echo intensity ratio of the two maxima was independent of temperature as shown in Figure 5. Since both the  $S=1/2$  and  $S=1$  molecules are magnetically isolated, the contributions of the two species to the echo intensity  $I(S)$  can

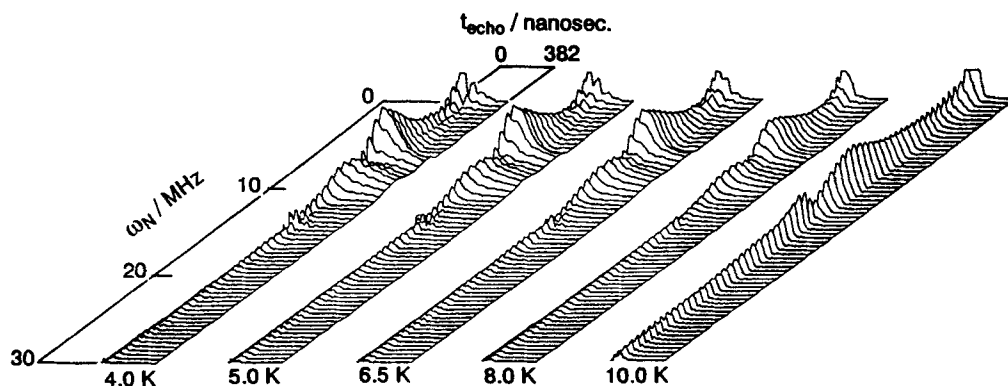


FIGURE 5 Two-dimensional representation of the echo-detected nutation spectra. The echo signals  $S(t_p, t_{\text{echo}})$  were Fourier-transformed along the  $t_p$ -axis into the frequency ( $\omega_N$ )-domain power spectra. In order to obtain a better S/N ratio, a higher power was applied at 10.0 K than at lower temperatures (+ 5 dB).

simply be expressed in terms of temperature for  $T \ll 2J/k_B$  as

$$I(S=1) \propto (1/T)\exp(2J/k_B T), \quad (2)$$

$$I(S=1/2) \propto 1/T. \quad (3)$$

Therefore, the echo intensity ratio should be given by

$$I(S=1)/I(S=1/2) \propto \exp(2J/k_B T). \quad (4)$$

This temperature dependence has not been observed in the present experiment. The nutation spectra failed to reflect the magnetization values of the two spin species quantitatively as a function of temperature. A possible origin of the deviation of the intensity ratio from the above model is ascribed to the difference in the relaxation times of the two species which determine the echo intensity in the nutation spectrum. It is noteworthy that the relaxation for an excitation period of  $t_p$  has been neglected in the theory. The effect of the detection method (FID- or echo-detection) on the signal intensity in the Fourier-transformed nutation spectrum should also be responsible; the method used in this study is not a genuine "transient" but an "indirect" one through the echo signals. The correspondence of nutation signal intensity with static susceptibility should be examined further in other model systems with various  $J/k_B T$  values and underlying relaxation mechanisms.

In conclusion, the echo-detected nutation method has been applied to a crystalline solid of an organic biradical, *p*-BNN. It was found that the nutation experiment can facilitate the spectroscopic identification of two different paramagnetic species,  $S=1$  and  $S=1/2$ . This finding showed the applicability of the method to molecular magnetic materials; its advantage in discriminating between different spin quantum numbers was demonstrated. It was also pointed out that quantitative aspect of the nutation spectroscopy, particularly its intensity analysis, is an open problem for further investigations to establish the methodology.

### ACKNOWLEDGMENT

This work has been supported by Grant-in-Aid for Scientific Research on Priority Area "Molecular Magnetism" (Area No. 228/04 242 103) from the Ministry of Education, Science and Culture, Japan. The authors are grateful to Professor A. Schweiger (E. T. H., Zürich) and Professor J. Isoya (University of Library and Information Science, Ibaraki) for their stimulating suggestions.

## REFERENCES

1. H. C. Torrey, Phys. Rev., **76**, 1059(1949).
2. I. Solomon, Phys. Rev. Lett., **2**, 301(1959).
3. C. S. Yannoni and R. D. Kendrick, J. Chem. Phys., **74**, 747(1981).
4. A. Samoson and E. Lippmaa, Chem. Phys. Lett., **100**, 205(1982).
5. A. Samoson and E. Lippmaa, Phys. Rev. B, **28**, 6567(1983).
6. F. M. M. Geruts, A. P. M. Kenthens and W. S. Veeman, Phys. Lett., **120**, 206(1985).
7. A. P. M. Kenthens, J. J. M. Lemmens, F. M. M. Geruts and W. S. Veeman, J. Mag. Reson., **71**, 62(1987).
8. R. Janssen, G. H. A. Tjink and W. S. Veeman, J. Chem. Phys., **88**, 518(1988).
9. R. Janssen and W. S. Veeman, J. Chem. Soc. Faraday Trans., **84**, 3747(1988).
10. J. Isoya, H. Kanda, J. R. Norris, J. Tang and M. K. Bowman, Phys. Rev. B, **41**, 3905(1990).
11. A. V. Astashkin and A. Schweiger, Chem. Phys. Lett., **174**, 595(1990).
12. K. Sato, D. Shiomi, T. Takui, K. Itoh, T. Kaneko, E. Tsuchida and H. Nishide, J. Spectrosc. Soc. Jpn., **43**, 280(1994).
13. T. Takui, K. Sato, D. Shiomi, K. Itoh, T. Kaneko, E. Tsuchida and H. Nishide, Proceedings of this conference.
14. D. Shiomi, Dr. Thesis, University of Tokyo (1993).
15. D. Shiomi, M. Tamura, H. Sawa, R. Kato and M. Kinoshita, Synth. Metals, **56**, 3279(1993).
16. A. Caneschi, P. Chiesi, L. David, F. Ferraro, D. Gatteschi and R. Sessoli, Inorg. Chem., **32**, 1445(1993).
17. E. F. Ullman, J. H. Osiecki, D. G. B. Boocock and R. Darcy, J. Am. Chem. Soc., **94**, 7049(1972).
18. J. A. D'Anna and J. H. Wharton, J. Chem. Phys., **53**, 4047(1970).
19. C. P. Keijzers, E. J. Reijerse and G. Schmidt, in Pulsed EPR: A new field of applications, (North Holland, Amsterdam, 1989), p.15.
20. For example, see I. M. Brown, J. Chem. Phys., **55**, 2377(1971).